

Thermodynamic models of low temperature Mn-Ni-Si precipitation in reactor pressure vessel steels

Wei Xiong ^a, Huibin Ke ^a, Peter Wells ^b, Leland Barnard ^c,

Ramanathan Krishnamurthy ^a, G. Robert Odette ^{b,d}, Dane Morgan ^{a,c,*}

^a Department of Materials Science and Engineering, University of Wisconsin, Madison, WI 53706, USA

^b Materials Department, University of California, Santa Barbara, CA 93106, USA

^c Materials Science Program, University of Wisconsin, Madison, WI 53706, USA

^d Mechanical Engineering, University of California, Santa Barbara, CA 93106, USA

* Corresponding author:

Dane Morgan: ddmorgan@wisc.edu, 608-265-5879

Abstract: Large volume fractions of Mn-Ni-Si (MNS) precipitates formed in irradiated light water reactor pressure vessel (RPV) steels cause severe hardening and embrittlement at high neutron fluence. A new equilibrium thermodynamic model was developed based on the CALPHAD method using both commercial (TCAL2) and specially assembled databases to predict precipitation of these phases. Good agreement between the model predictions and experimental data suggest that equilibrium thermodynamic models provide a basis to predict terminal MNS precipitation over wider range of alloy compositions and temperatures, and can also serve as a foundation for kinetic modeling of precipitate evolution.

Keywords: nuclear materials, phase equilibria, simulation

Irradiation enhanced precipitation hardening is the primary cause of in-service embrittlement of reactor pressure vessel (RPV) steels. Odette and collaborators long ago predicted that at very high fluence Mn-Ni-Si (MNS), so called late blooming phases, would form large mole fractions of nano-scale precipitates, even in low Cu RPV steels [1–6]. These early predictions have since been qualitatively confirmed and refined [2,3,7,8]. Since MNS precipitates could result in severe and unanticipated embrittlement, and they are not treated in current regulatory models, these precipitates may limit currently planned plant life extension of up to 80 or more years. They are therefore arguably the most immediately important reactor materials aging-degradation challenge facing nuclear power’s continued carbon-free contribution to our electricity supply [1,9]. MNS precipitates do not develop under typical thermal aging conditions at temperatures relevant to LWR operation (523-573K) due to very slow thermal diffusion kinetics. However, they have been observed following irradiation and, most recently, in high Cu and Ni alloys after very long time thermal aging at higher temperatures [10]. The challenge of producing these phases in the absence of irradiation has led to significant debate in the literature about the thermodynamic stability of MNS features and their potential for forming large precipitate mole fractions.

Previous first principles and atomistic model calculations predicted only small volume fractions of non-equilibrium Mn-Ni clusters [11]; or, most recently, a possible equilibrium Mn-Ni phase, but only under very restricted composition and temperature conditions [12]. Thus the thermodynamic stability of MNS precipitates at RPV steel compositions and temperatures remains a critically important open question. This paper presents the first rigorous and quantitative systematic general model of MNS precipitate thermodynamics. The most important findings are that known equilibrium intermetallic MNS phases are thermodynamically stable in dilute Fe-Mn-Ni-Si alloys at RPV relevant temperatures and that our thermodynamic models can be used to predict precipitate mole fraction for highly

irradiated materials. The models therefore provide a basis to predict MNS mole fraction, and therefore hardening and embrittlement, for irradiated steels over a wide range of compositions and temperatures. Furthermore, the models also establish a robust, empirically informed foundation to develop non-equilibrium kinetics models.

It is important to note that MNS precipitates form in both Cu-free and Cu-bearing steels [3,11] and that we believe the present models, which exclude Cu, are applicable in both cases. In the case of Cu bearing alloys, coherent Cu-Mn-Ni-Si precipitates first nucleate and grow very rapidly. The rapid evolution is driven by the high supersaturation of Cu. Subsequently, the MNS precipitates continue to grow as a nearly Cu-free appendage co-precipitated MNS phase. Essentially pure MNS precipitates also form in very low and Cu free steels, with compositions very similar to the MNS co-precipitate appendages. Thus the experiments suggest that Cu primarily plays a catalyzing role in accelerating MNS phase formation but does not alter the nature of the MNS precipitates. Therefore, the present models without Cu explicitly included in the precipitate thermodynamics can be expected to apply to both Cu-free and Cu-bearing steels.

Embrittlement data for realistic reactor service conditions at low flux (neutrons/m²-s) and high, extended life fluence (neutrons/m²) are not available. Therefore, robust predictions will require accurate computational models for MNS precipitate evolution as a function of the combination of material and irradiation variables. In comparing our thermodynamic models to experiments we assume that: (i) irradiation primarily affects the kinetics of the precipitation by irradiation enhanced diffusion due to excess vacancies produced by displacement damage [5,6,13]; and (ii) at a sufficiently high fluence the precipitates approach an equilibrium phase separated state. Under these assumptions the precipitate mole fractions and compositions in highly irradiated alloys can be compared to the equilibrium thermodynamic predictions. This modeling approach is in contrast to the hypothesis that

MNS precipitates are stabilized by non-equilibrium radiation induced effects, rather than as the result of near equilibrium thermodynamics accelerated by radiation enhanced diffusion [11]. We show below that the model predictions are consistent with the recent experimental atom probe tomography (APT) results reported by Wells et al. and strongly suggest that intermetallic MNS phases are thermodynamically stable in dilute quaternary Fe-Mn-Ni-Si alloys at low temperatures [14]. Since these new experimental results are under submission, we briefly summarize them in the Supplemental Materials.

The CALPHAD method was adopted to predict the equilibrium MNS phases, mole fractions and compositions in the quaternary Fe-Mn-Ni-Si system for six different RPV steels (denoted LC, LD, LG, LH, LI, and CM6) associated with the APT results cited above [14]. The alloys investigated cover a wide and systematic range of Cu and Ni contents, along with smaller variations in Mn and Si, as shown in Table 1. The alloys were irradiated at an accelerated flux of $\approx 2.3 \times 10^{14}$ n/cm²-s to a high fluence of 1.1×10^{21} n/cm² in the Idaho National Laboratory Advanced Test Reactor (ATR) at 563K. The alloy compositions are the average bulk values measured by APT. The corresponding precipitate compositions, also shown in TABLE S1, are the averages for many individual solute clusters. It should be noted that APT cannot characterize the structure of the precipitates.

We employed two thermodynamic databases for the CALPHAD modeling in order to help establish the sensitivity of the predictions to the detailed free energy model. The first database was constructed from the literature, which we refer as the UW1 database, and the parameters regarding it are listed in TABLE S2. It is based on a simplified thermodynamic treatment to avoid the efforts required to build a complete multicomponent Mn-Ni-Si-Fe database. The UW1 database combines previously established Mn-Ni-Si intermetallic phase descriptions [15] and the corresponding thermodynamics of dilute solid solution bcc Fe-X binaries (X= Mn, Ni, Si), also obtained from CALPHAD models [16–18]. The second

database is the commercial TCAL2 database [19], implemented in the Thermo-Calc software package. TCAL2 was chosen as it is the only Thermo-Calc database that currently contains a comprehensive thermodynamic description for all of the ternaries in the Fe-Mn-Ni-Si system [19] over the entire range of relevant compositions and temperatures.

Most notably, both UW1 and TCAL2 databases independently predict precipitation of MNS phases which are compositionally similar to those observed by APT [14]. Although the UW1 database is based on a relatively simplified thermodynamic model, it has the advantage that all the parameters are openly accessible and modifiable. It is therefore flexible and can be readily improved, e.g. by adjusting parameters, extending to include more alloying elements, and integrating with kinetic and more complex phase diagram models. The more extensive and validated TCAL2 database is here considered a highly vetted benchmark for the MNS precipitation model.

In the case of the UW1 database, the binary bcc phases are extrapolated into the ternary and quaternary systems using the Muggianu symmetric methods [20,21]. There are 12 known ternary phases in the Mn-Ni-Si system, which are all included in the UW1 database as potential precipitates. The CALPHAD-type thermodynamic parameters of these phases are directly taken from the descriptions published by Hu et al. [15]. We consider a temperature of 550K, which is relevant for RPV operating conditions and close to the nominal irradiation temperature of $\approx 563\text{K}$ used in the comparison irradiation experiments (see Supplemental Materials). There are 7 ternary phases in the isothermal section at 550 K, as shown in FIG. 1. Using the CALPHAD nomenclature, the ternary T3, T7, T9 and T10, are considered as stoichiometric compounds, while T6 and T8 have a finite range of compositions (phase field), represented by slightly heavier green lines in FIG. 1. Structural information regarding these phases can be found in Ref [15]. The T6 phase, which is particularly relevant, has a constant 33.3% Mn composition and a range of Si from 12.7 to

20.7% and a corresponding Ni range of 46.0 to 54.0%, represented by a composition in the form of $Mn(Ni_xSi_{1-x})_2$.

The composition and phase selection results are summarized in FIG. 1 and TABLE S1. Note that, as discussed above, the Cu content of the precipitates is not modeled as we believe it does not impact the final precipitate mole fraction, phase selection, or composition.

It is useful to consider how the bulk alloy compositions influence the observed phase selection and precipitate chemistry. Both the predicted and experimental precipitate compositions increase and decrease in similar directions to that of the bulk alloys. The experimental results show medium Ni (0.7-0.8%) and Si (0.42-0.43%) LG, LH, LI, LC series alloys all yield precipitates that cluster around the T6 phase field composition, but near the higher Si terminus. The higher Ni (1.18%) and Si (0.54%) alloy LD contains precipitates with higher enrichment in these elements near the T3 phase composition. The very high Ni (1.69%) and Mn (1.42% versus an average of $1.05 \pm 0.18\%$ in the other steels) and lower Si (0.39%Si) Cu free CM6 alloy shifts the corresponding precipitate composition to slightly higher Ni and lower Si, near the predicted T6 phase. The model predictions generally follow qualitatively similar trends. However, only T6, with a narrow range of composition, is predicted by UW1 model. The TCAL2 model predicts that the T6 (33%Mn) phase fraction increases, while the T3 (21%Mn) fraction decreases with increasing alloy Mn contents: the TCAL2 model predicts the lowest Mn alloy LG (0.87%Mn) is 100% T3, while highest Mn alloy CM6 (1.42%Mn) is 100% T6.

FIG. 2 shows a stacked Si, Mn, Ni mole fraction bar chart for the various alloys (the equivalent numerical data is summarized in TABLE S1). We find that both databases reasonably predict the typical compositions and mole fractions of the precipitates, which are approximately 20%Si, 30%Mn and 50%Ni, within $\pm 10\%$. The predictions of the UW1 database for precipitate content of Mn and Ni are closer to experiment than the TCAL2

database, while the latter yields generally closer predictions of the Si contents. The maximum and root-mean-square difference between the experiments and the database predictions for total precipitate mole fraction (as a percentage of the experimental values) are 19% and 14% for TCAL2 and 15% and 12% for UW1, respectively. While these results cannot be used to conclude that one database is inherently superior to the other, the broad agreement between both and the experimental data suggest that the experimentally observed phase separation is closely approaching equilibrium, and that this equilibrium is well represented by both databases. We also generally find the precipitate mole fraction scales approximately linearly with the alloy mole fraction of Ni, Mn, and Si (FIG. S1) and with the Ni content (FIG. S2) [14]. As seen in FIG. S1, the total fraction of the solutes that precipitate increases with total solute fraction and Ni, ranging from a low of about 50% at an intermediate Ni levels to about 75% at the highest alloy content of this element. These results also indicate the broad consistency of the volume fractions of MNS precipitates between fully independent APT measurements and model predictions.

Despite the generally similar overall compositions, different phases are predicted by the two databases for five of the six alloys. TCAL2 predicts both T3 and T6 for LC, LD, LH and LI and 100% T3 for LG, while UW1 predicts 100% T6 for all alloys. These differences reflect the sensitivity of the results to the CALPHAD model parameterization, where small free energy differences lead to altered phase selection for similar (or even the same) starting alloy compositions. The differences in the predicted compositions compared to the APT compositions is therefore almost certainly, at least in part, due to limited accuracy of the thermodynamic models; this conclusion is supported by the disagreement between the thermodynamic models themselves.

Note our results are broadly consistent with earlier thermodynamically based models of Odette and co-workers [3–5]. However, they differ from the recent conclusions of Happy et

al [11], who used first principle bonding energy calculations and Monte Carlo simulations to predict rapid formation of tiny, non-equilibrium, Mn-Fe self-interstitial atom defect clusters, containing small amounts of Ni. These clusters quickly form and are enriched in Mn due to radiation induced segregation (RIS). These authors reject the existence of any thermodynamic phases, since they find the Mn-Ni interaction is repulsive; and they suggest that a third element is unlikely to alter this conclusion. Bonny et al. [12] used similar computational tools to determine that coherent Mn-Ni precipitates (B2) can form thermodynamically, but under such limited temperature-composition conditions that any large volume fraction would have to be caused by RIS. Thus both of these papers are at odds with our current results and experimental observations [14]. However, more detailed discussion of the reasons for these differences is beyond the scope of this letter.

Overall, the model-experiment consistency is quite remarkable. Even if the models perfectly reflected the thermodynamics of the Ni-Mn-Si bulk system in equilibrium with Fe, it cannot be expected that this would translate to exact models of precipitates in the Fe-Ni-Mn-Si(-Cu) system under irradiation. Complicating factors not included in the bulk thermodynamic models include significant interface and potential coherency strain sources of free energy, complex core-shell structures [3], nonequilibrium effects (e.g., radiation-induced solute segregation), and possible unmodeled effects of evolution under irradiation (e.g., interstitial contributions). However, our results suggest the important fact that these additional factors beyond bulk thermodynamics collectively have a rather modest influence on the precipitate phase selection, composition and mole fraction. Further verification of these conclusions will require precise identification of the actual precipitate intermetallic phases and their structures.

In summary, this work predicts that Mn-Ni-Si (MNS) precipitates will eventually form in RPV alloys at reactor relevant temperatures due their being stable thermodynamic phases.

Further, the model supports the conclusion that the composition of MNS precipitates, and the corresponding mole fractions, in RPV alloys under high-fluence irradiation conditions are governed largely by near equilibrium bulk thermodynamics. Our results also show that a freely available, flexible, and simple thermodynamic database compiled by us from available CALPHAD assessments (UW1) can provide predictions broadly comparable to that of the commercial TCAL2 database, both of which well predict the typical composition range and the total solute mole fractions (\approx volume fraction) of the MNS precipitates. The verified model provides a basis to predict equilibrium phases over a wide-range of alloy compositions and temperatures that can, and will, be further tested and refined by mechanistically guided experiments.

The predicted volume fractions can be directly used to estimate mechanical property changes [14]. Most notably these results support the hypothesis that Mn-Ni-Si phases could lead to enormous hardening, and correspondingly severe embrittlement, under some extended life light water reactor service conditions. These models also provide a powerful thermodynamic foundation for more complete kinetic simulations of precipitate evolution, and other non-equilibrium phenomena, such as solute segregation, heterogeneous nucleation, and chemically complex MNS precipitate structure.

Future work will refine the CALPHAD models developed here through comparison with experimental long-term annealing studies to probe the corresponding precipitate phase boundaries.

Acknowledgements

This research is being performed using funding received from the DOE Office of Nuclear Energy's Nuclear Energy University Program at UW (NEUP 10-888) and at UCSB (NEUP 3176). We would like to acknowledge Randy Nanstad and Jeremy Busby of Oak Ridge National Laboratory, and the U.S. Department of Energy Office of Nuclear Energy's Light

Water Reactor Sustainability Program, Materials Aging and Degradation Pathway for additional support for Huibin Ke. Support for the irradiations that provided the data cited here, but reported separately, was provided by the INL ATR National Scientific Users Facility.

References

- [1] G.R. Odette, and G.E. Lucas: Embrittlement of nuclear reactor pressure vessels. *JOM J. Miner. Met. Mater. Soc.* **53**(7), 18 (2001).
- [2] G.R. Odette, and R.K. Nanstad: Predictive Reactor Pressure Vessel Steel Irradiation Embrittlement Models : Issues and Opportunities. *JOM J. Miner. Met. Mater. Soc.* **61**(7), 17 (2009).
- [3] C.L. Liu, G.R. Odette, B.D. Wirth, and G.E. Lucas: A lattice Monte Carlo simulation of nanophase compositions and structures in irradiated pressure vessel Fe-Cu-Ni-Mn-Si steels. *Mater. Sci. Eng. A* **238**, 202 (1997).
- [4] G.R. Odette: Radiation Induced Microstructural Evolution In Reactor Pressure Vessel Steels, in Materials Research Society Symposium Proceedings, edited by I.M. Robertson, L.E. Rehn, S.J. Zinkle, and W.J. Phythian, (Materials Research Society, Warrendale, 1995), pp. 137–148.
- [5] G.R. Odette, and G.E. Lucas: Recent progress in understanding reactor pressure vessel steel embrittlement. *Radiat. Eff. Defects Solids* **144**(1), 189 (1998).
- [6] G.R. Odette, and B.D. Wirth: A computational microscopy study of nanostructural evolution in irradiated pressure vessel steels. *J. Nucl. Mater.* **251**, 157 (1997).
- [7] M.K. Miller, A.A. Chernobaeva, Y.I. Shtrombakh, K.F. Russell, R.K. Nanstad, D.Y. Erak, and O.O. Zabusov: Evolution of the nanostructure of VVER-1000 RPV materials under neutron irradiation and post irradiation annealing. *J. Nucl. Mater.* **385**(3), 615 (2009).
- [8] M.K. Miller, and K.F. Russell: Embrittlement of RPV steels: An atom probe tomography perspective. *J. Nucl. Mater.* **371**(1-3), 145 (2007).
- [9] G.R. Odette, M.J. Alinger, and B.D. Wirth: Recent Developments in Irradiation-Resistant Steels. *Annu. Rev. Mater. Res.* **38**(1), 471 (2008).
- [10] P.D. Styman, J.M. Hyde, K. Wilford, a. Morley, and G.D.W. Smith: Precipitation in long term thermally aged high copper, high nickel model RPV steel welds. *Prog. Nucl. Energy* **57**, 86 (2012).
- [11] R. Ngayam-Happy, C.S. Becquart, C. Domain, and L. Malerba: Formation and evolution of MnNi clusters in neutron irradiated dilute Fe alloys modelled by a first principle-based AKMC method. *J. Nucl. Mater.* **426**(1-3), 198 (2012).
- [12] G. Bonny, D. Terentyev, a. Bakaev, E.E. Zhurkin, M. Hou, D. Van Neck, and L. Malerba: On the thermal stability of late blooming phases in reactor pressure vessel steels: An atomistic study. *J. Nucl. Mater.* **442**(1-3), 282 (2013).
- [13] G.R. Odette, T. Yamamoto, and D. Klingensmith: On the effect of dose rate on irradiation hardening of RPV steels. *Philos. Mag.* **85**(4-7), 779 (2005).
- [14] P. Wells, Y. Wu, T. Milot, G.R. Odette, T. Yamamoto, and B. Miller: Atom probe studies of the nano-scale Mn-Ni-Si precipitates for RPV steels under irradiation. *Submitted to Acta Mater.* (n.d.).

- [15] B. Hu, H. Xu, S. Liu, Y. Du, C. He, C. Sha, D. Zhao, and Y. Peng: Experimental investigation and thermodynamic modeling of the Mn–Ni–Si system. *Calphad* **35**(3), 346 (2011).
- [16] J. Lacaze, and B. Sundman: An assessment of the Fe-C-Si system. *Metall. Trans. A* **22**(10), 2211 (1991).
- [17] C. Servant, B. Sundman, and O. Lyon: Thermodynamic assessment of the Cu-Fe-Ni system. *Calphad* **25**(1), 79 (2001).
- [18] W. Huang: An assessment of the Fe-Mn system. *CALPHAD* **13**(3), 243 (1989).
- [19] The TCS Al-based alloy database, TCAL2. Version 2.0. Stockholm: Thermo-Calc SofAB; 2013. *The TCS Al-Based Alloy Database, TCAL2. Version 2.0. Stockholm: Thermo-Calc Software AB*; (2013).
- [20] Y.-M. Muggianu, M. Gambino, and J.-P. Bros: Enthalpy of formation of liquid bismuth-gallium-tin alloys at 723K. Choice of an analytical representation of integral and partial thermodynamic function of mixing. *J. Chim. Phys. Physico-Chimie Biol.* **72**, 83 (1975).
- [21] M. Hillert: The compound energy formalism. *J. Alloys Compd.* **320**(2), 161 (2001).

List of Figures

1. Isothermal section of the Mn-Ni-Si system at 550 K. Black solid symbols are compositions of precipitates from experiment, blue symbols (open dark grey) are the calculated compositions of precipitates from the UW1 database, and red symbols (open light grey) are the calculated compositions of precipitates from the TCAL2 database.
2. Comparison of mole fraction of different elements in precipitates observed by Atom Probe Tomography (APT) and predicted by UW1 and TCAL2 database. The numbers shown above each set of column are the bulk Cu and Ni composition (at.%) of each alloy.

Table 1. Bulk composition of alloys derived from Atom Probe Tomography. Fe is balance.

Alloy No.	Bulk Composition (at. %)							
	Mn	+/-	Ni	+/-	Si	+/-	(Cu)	(+/-)
LC	1.16	0.01	0.80	0.03	0.43	0.02	0.28	0.01
LD	1.08	0.08	1.18	0.05	0.54	0.02	0.25	0.02
LG	0.87	0.07	0.71	0.01	0.43	0.01	0.00	0.00
LH	1.19	0.06	0.73	0.02	0.42	0.01	0.08	0.00
LI	0.97	0.10	0.70	0.01	0.42	0.01	0.15	0.00
CM6	1.42	0.03	1.69	0.04	0.39	0.01	0.00	0.00

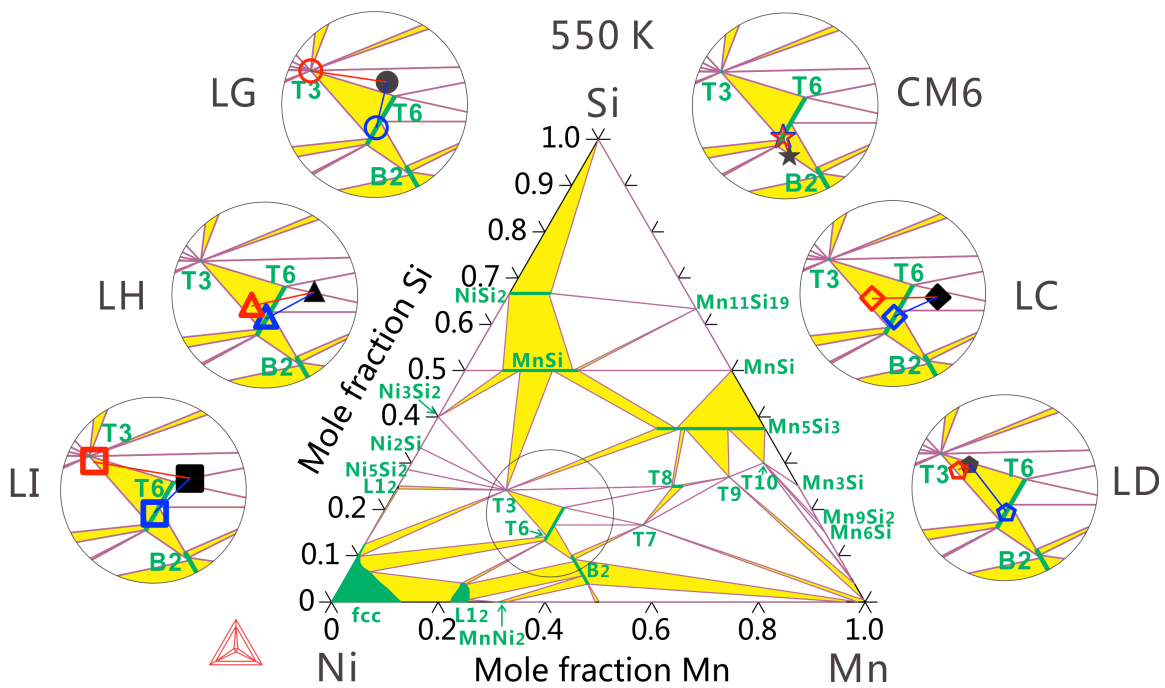


FIG. 1. Isothermal section of the Mn-Ni-Si system at 550 K. Black solid symbols are compositions of precipitates from experiment, blue symbols (open dark grey) are the calculated compositions of precipitates from the UW1 database, and red symbols (open light grey) are the calculated compositions of precipitates from the TCAL2 database.

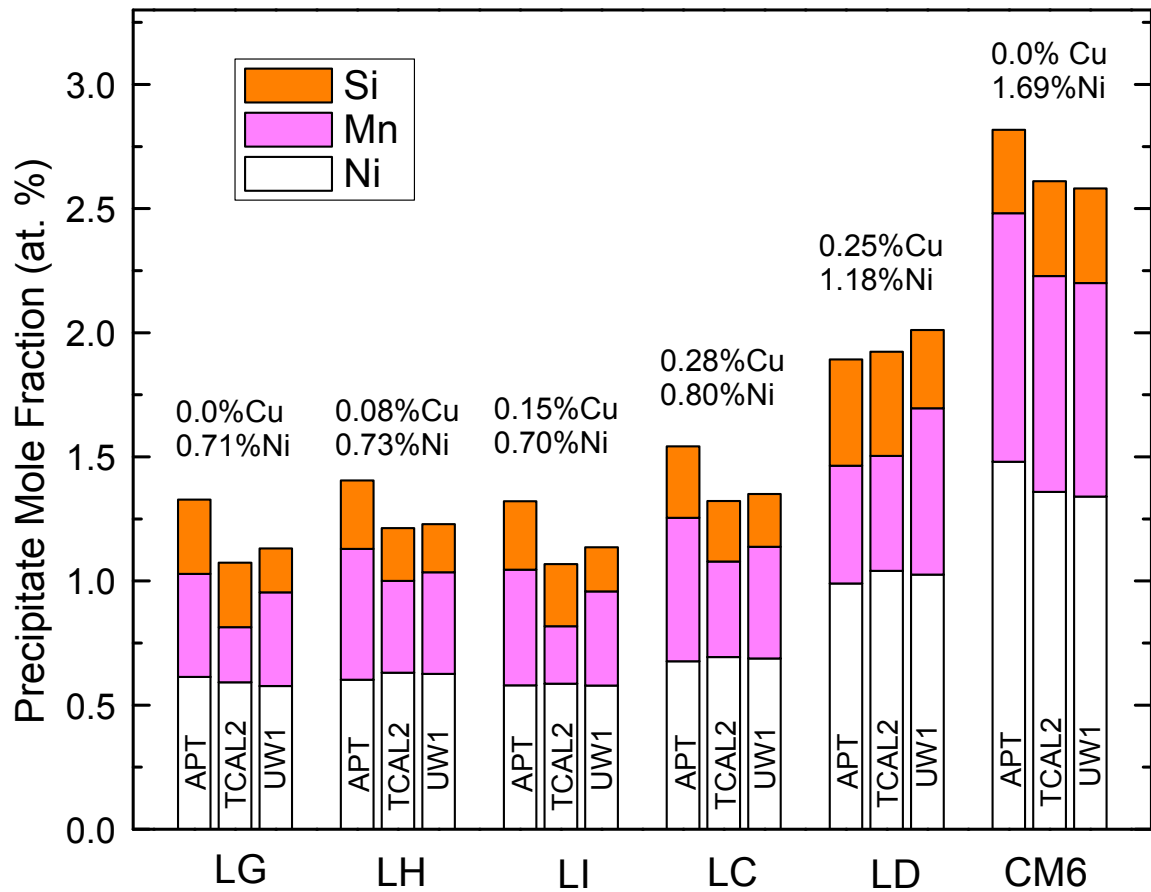


FIG. 2. Comparison of mole fraction of different elements in precipitates observed by Atom Probe Tomography (APT) and predicted by UW1 and TCAL2 database. The numbers shown above each set of column are the bulk Cu and Ni composition (at.%) of each alloy.